

Magnetoresistance, micromagnetism, and domain-wall scattering in epitaxial hcp Co films

U. Rüdiger and J. Yu

Department of Physics, New York University, 4 Washington Place, New York, New York 10003

L. Thomas and S. S. P. Parkin

IBM Research Division, Almaden Research Center, San Jose, California 95120

A. D. Kent*

Department of Physics, New York University, 4 Washington Place, New York, New York 10003

Large negative magnetoresistance (MR) observed in transport measurements of hcp Co films with stripe domains were recently reported and interpreted in terms of domain-wall (DW) scattering mechanism. Here detailed MR measurements, magnetic force microscopy, and micromagnetic calculations are combined to elucidate the origin of MR in this material. The large negative room-temperature MR reported previously is shown to be due to ferromagnetic resistivity anisotropy. Measurements of the resistivity for currents parallel (CIW) and perpendicular to DW's (CPW) have been conducted as a function of temperature. Low-temperature results show that any intrinsic effect of DW's scattering on MR of this material is very small compared to the anisotropic MR.

The effect of magnetic domain walls (DW's) on the transport properties of thin films and nanostructures is a topic of great current interest. Recent experimental research has extended early studies of iron single crystals^{1,2} to nanofabricated thin-film structures of 3d transition metals³⁻⁵ and transition-metal alloys.^{6,7} This topic has been approached from a number of viewpoints. In nanowires an experimental goal has been to use magnetoresistance (MR) to investigate DW nucleation and dynamics in search of evidence for macroscopic quantum phenomena. Conductance fluctuations and MR hysteresis observed at low temperature in nanowires of Ni, Fe, and Co (Refs. 8 and 9) have stimulated theoretical work on the effect of DW's on quantum transport in mesoscopic ferromagnetic conductors.^{10,11} In thin films and microstructures with stripe domains, experiments have focused on understanding the basic mechanisms of DW scattering of conduction electrons. Specifically, large negative MR observed at room temperature in hcp Co thin films with stripe domains were recently reported and interpreted in terms of a giant DW scattering contribution to the resistivity.⁴ Independently, and to understand this result, a mechanism of DW scattering was proposed which invokes the two channel model of conduction in ferromagnets and spin dependent electron scattering—a starting point for understanding the phenomena of giant MR (GMR).¹² Within this model DW's increase resistivity because they mix the minority and majority spin channels and thus partially eliminate the short circuit provided by the lower resistivity spin channel in the magnetically homogeneous ferromagnet.

Here we present a physical interpretation of the MR of hcp Co films with stripe domains which is based on both experimental results and micromagnetic modeling. We have conducted experiments on samples of systematically varied magnetic structure and DW density and as a function of the angle of the transport current with respect to DW's. The role of conventional sources of MR in ferromagnetic metals on the interpretation of such experiments is discussed in detail. MR measurements, magnetic force microscopy (MFM) im-

aging in conjunction with micromagnetic simulations show that the large negative MR observed at room temperature in hcp Co films for fields applied parallel to the the easy magnetic axis is due mainly to a conventional anisotropic transport effect in ferromagnetic metals, not large DW scattering effects.

Epitaxial (0001) oriented hcp Co films of 55, 70, 145, and 185 nm thicknesses have been studied. The films were grown on *a*-axis (11 $\bar{2}$ 0) sapphire substrates using *e*-beam evaporation techniques under UHV conditions. First, at a temperature of 680 K a 10-nm-thick (0001) Ru seed layer was deposited followed by a (0001) Co layer. The Co layer was protected against corrosion by a 5-nm-thick Ru capping layer. X-ray $\theta/2\theta$ scans indicate *c*-axis orientation of the Ru and Co layers. Off-axis x-ray pole figures show that the films are also oriented in plane with respect to the sapphire substrate. The films were patterned using projection optical lithography and ion milling in order to produce microstructures of well defined geometry for MR studies. A residual resistivity of $\rho = 0.16 \mu\Omega \text{ cm}$ and the residual resistivity ratio of 19 for a 185-nm-thick 5 μm linewidth Co wire confirm the high crystalline quality of the films.

These films have a strong uniaxial anisotropy with the magnetic easy axis perpendicular to the film plane.¹³ The competition between magnetostatic, exchange, and magnetocrystalline energies leads to stripe domain configurations in which the domain size depends on the sample thickness and the domain configurations depend on the sample magnetic history. Figure 1 shows MFM images of a 70-nm-thick 5- μm -linewidth Co wire in zero magnetic field. These MFM images, taken with a vertically magnetized magnetic tip, highlight the out-of-plane component of the wire magnetization. Images are shown after magnetic saturation: (a) perpendicular to the film plane, (b) in plane and transverse to the wire axis, and (c) in plane and along the wire axis. As seen in Fig. 1, an in-plane applied field can be employed to align DW's in stripes.¹⁴ Figures 1(b) and 1(c) show that DW's can be oriented parallel or perpendicular to the long axis of the

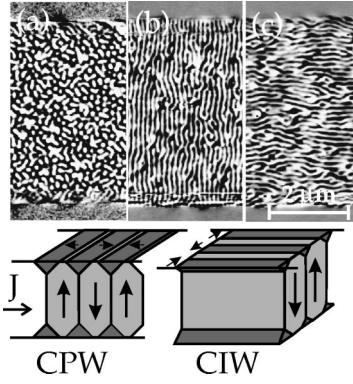


FIG. 1. MFM images in zero applied field of a of 5- μm -linewidth 70-nm-thick Co wire after (a) perpendicular, (b) transverse, and (c) longitudinal magnetic saturation. The model shows the orientation of stripe and flux closure caps with respect to the current for (b) CPW and (c) CIW geometries.

wire and thus the applied current, denoted as current-in-wall (CIW) and current-perpendicular-to-wall (CPW) geometries, respectively¹² (as shown in the drawing in Fig. 1).

Modeling of the film micromagnetic structure is essential to understand the MR results. An important parameter for stripe domain materials is the ratio of anisotropy to demagnetization energy, known as the quality factor Q , given by $Q = K/2\pi M_s^2$.^{15–17} For small Q ($Q \ll 1$), the magnetostatic energy dominates the anisotropy energy. In this limit, it is energetically favorable to maintain flux closure at the film boundaries via the formation of closure domains (with magnetization parallel to the film surface) at the top and bottom film surfaces. In the limit of large Q ($Q \gg 1$), stripe domains with magnetization perpendicular to the surface are favored, leading to surface magnetic charges. Since hcp Co has an intermediate Q value ($Q = 0.35$), numerical modeling of the film micromagnetic structure is necessary to determine equilibrium domain configurations. It has been shown numerically that in hcp Co DW's branch, being Bloch-like in the film center and forming flux closure caps at the top and bottom surface of the film to reduce the magnetostatic energy.¹⁸

The magnetic structure of films of the thicknesses studied has been computed in zero field with the LLG Micromagnetics Simulator.¹⁹ The equilibrium magnetization is found from the minimization of the system's free energy composed of exchange, magnetocrystalline anisotropy, magnetostatic, and Zeeman terms. The time evolution of the magnetization is given by the Landau-Lifschitz-Gilbert equation.²⁰ The magnetization distribution is approximated by a discrete cubic mesh, with a cell volume of 1000 nm³ and tests performed using a finer grid have shown similar results. As seen in Fig. 2(a), such calculations produce domain widths which are in good agreement with experiment. The inset of Fig. 2(b) shows a part of the simulated magnetic cross section of a 70-nm-thick Co element (with overall dimensions of 1500 \times 500 \times 70 nm), where the arrows indicate the magnetization direction of the stripe and flux closure caps. Flux closure caps constitute approximately 25% of the total wire volume, which is also an approximate measure of the in-plane magnetized volume. For all Co wire thicknesses investigated the closure cap volumes (in-plane magnetization) were calculated as shown on the left-hand axis of Fig. 2(b). By increas-

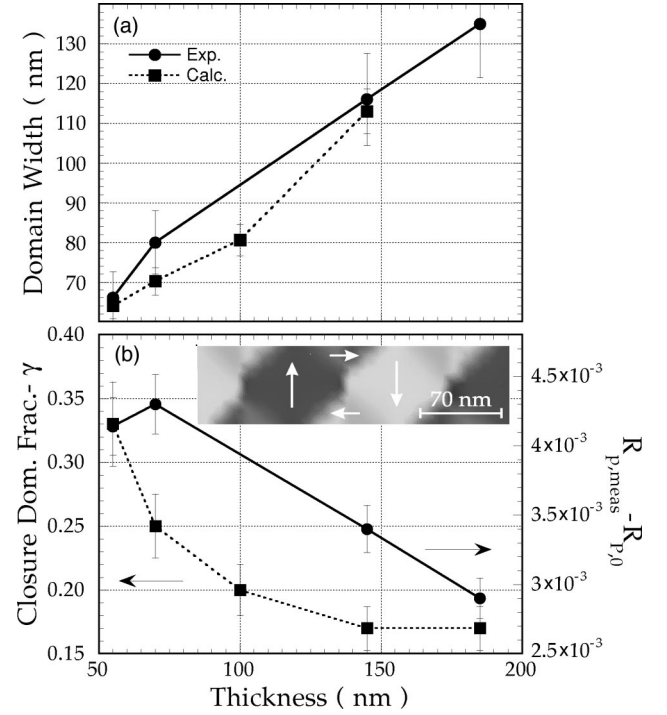


FIG. 2. (a) Domain size versus film thickness; experimental (solid circles) and calculated values (solid squares). (b) The calculated in-plane magnetization volume (solid squares) and the magnitude of the MR $R_{p,meas} - R_{p,0}$ in the perpendicular geometry (solid circles) as a function of wire thickness. Inset: Calculated magnetic domain cross section of a 70-nm-thick Co element showing out-of-plane magnetized stripe domains and in-plane magnetized flux closure caps.

ing the wire thickness from 55 to 185 nm the in-plane magnetization volume decreases from 33 to 17%.

MR measurements were performed using a variable temperature high-field cryostat with *in situ* rotation capabilities. The resistivity of the Co wires was measured using a four-probe ac (~ 10 Hz) bridge technique with currents of 10–100 μA . The applied magnetic field was oriented in-plane both parallel (longitudinal geometry) and perpendicular (transverse geometry) to the long wire axis (i.e., the current direction) as well as perpendicular to the film plane (perpendicular geometry). Figure 3(a) shows such measurements performed at room temperature on a 55-nm-thick film. The low-field MR is positive for in-plane magnetic fields and negative for perpendicular applied fields. Hysteresis is also evident, particularly in the perpendicular MR, which correlates well with magnetization hysteresis loops (Fig. 4). Above the saturation field (~ 1.4 T) there is a large anisotropy of the resistivity, with the resistivity largest when the magnetization is in the film plane and parallel to the current. As generally observed in ferromagnetic materials, the resistivity depends on the angle of the current and magnetization as well as the angle the magnetization makes with respect to the crystallographic axes. These anisotropies have their origin in the spin-orbit interaction and the fact that the orbital moment depends on the orientation of the magnetization in the crystal.^{21,22}

This resistivity anisotropy is important in the interpretation of the low-field MR because the magnetization in zero applied field has components along all three dimensions. For

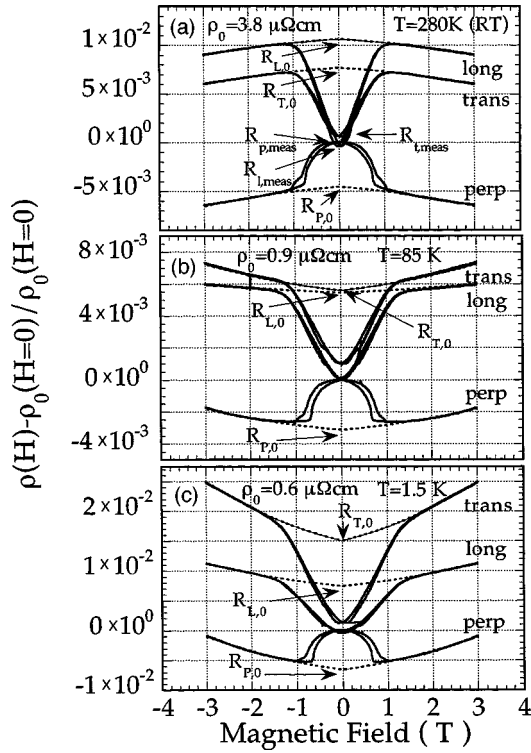


FIG. 3. MR data of a 5- μm -linewidth 55-nm-thick Co wire in the perpendicular, transverse, and longitudinal field geometries at (a) room temperature, (b) 85 K, and (c) 1.5 K.

example, for the CPW geometry (as illustrated in Fig. 1), the magnetization of the stripe domains are out-of-the-film plane and perpendicular to the current, the magnetization of the flux closure caps are in plane and parallel to the current, and the magnetization of the Bloch wall rotates through an orientation in plane and perpendicular to current. Thus a saturating field will both erase DW's and reorient the magnetization with respect to the current and crystal. The low-field MR which results from resistivity anisotropy and the reorientation of the film magnetization was neglected in the initial work on hcp Co films, as it was incorrectly assumed that the magnetization and current remain always perpendicular in zero applied field.⁴

This contribution can be estimated within an effective medium model of the resistivity. In the limit in which the elec-

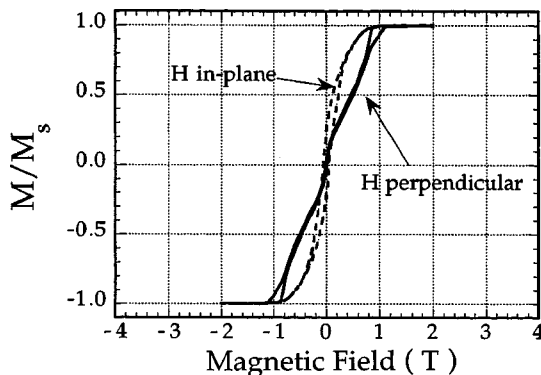


FIG. 4. Magnetization hysteresis loops measured with a superconducting quantum interference device magnetometer of a 55-nm-thick Co sample at 300 K for applied fields in plane (dashed line) and perpendicular to the film plane (solid line).

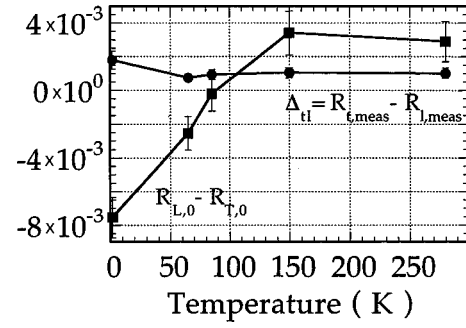


FIG. 5. Temperature dependence of difference between CPW and CIW resistivities, Δ_{tl} , and $R_{L,0} - R_{T,0}$ of a 55-nm-thick Co wire.

tron mean free path is smaller than the domain size²³ and the resistivity anisotropy is small, the resistivity can be written as a weighted average of the resistivities, to first order in the resistivity anisotropy, $\epsilon_L = R_{L,0} - R_{P,0}$ and $\epsilon_T = R_{T,0} - R_{P,0}$. Then starting from the maze configuration [Fig. 1(a)] the perpendicular MR is

$$R_{P,meas} - R_{P,0} = \gamma \left[\frac{1}{2} (R_{L,0} + R_{T,0}) - R_{P,0} \right] + O(\epsilon_L^2, \epsilon_T^2), \quad (1)$$

where γ is the volume of in-plane magnetized closure caps. Here $R_{L,T,P,0}$ are the MR extrapolated from high field to $H = 0$ (dashed lines in Fig. 3), as will be described below, and normalized to the resistivity measured at $H = 0$ in the maze configuration, $\rho_0(H = 0)$ ($R_{P,meas}$ is taken to be the zero of the MR, see Fig. 3). In this expression, the small volume of in-plane magnetized DW material has been neglected, only the flux closure caps are considered. Within this picture, the negative MR observed in the perpendicular field geometry is due to the erasure of higher resistivity closure caps in the applied field. Further, the magnitude of the perpendicular MR is thickness dependent because the volume of the in-plane magnetized material depends on sample thickness (Fig. 2). For example, from the MR measurements shown in Fig. 3(a) on a 55-nm-thick film and with $\gamma = 0.33$, $R_{P,0}$ is estimated to be -4.5×10^{-3} , in close correspondence with the measured perpendicular MR. Figure 2(b) shows that the perpendicular MR generally increases with increasing in-plane magnetized volume fractions. The difference between CPW and CIW resistivities (i.e., $R_{t,meas} - R_{l,meas}$), associated with rotating the magnetization direction of the flux closure caps from parallel (or antiparallel) to perpendicular to the current, in Fig. 3(a) is given by, $\gamma(R_{L,0} - R_{T,0}) = 1 \times 10^{-3}$, in close agreement with the experimental value. Such estimates show that the predominate MR effects observed in this material are explicable by film micromagnetic structure and resistivity anisotropy, without the need to invoke DW scattering effects.

Temperature-dependent resistivity measurements for CPW and CIW geometries show more interesting behavior, which is not explicable simply in terms of ferromagnetic resistivity anisotropy. With decreasing temperature the in-plane resistivity anisotropy changes sign,⁵ due to the increasing importance of the anisotropy in the Lorentz MR. The anisotropy of the Lorentz MR is important at low tempera-

TABLE I. Characteristics data for 5- μm -linewidth Co wires of 55, 70, 145, and 185 nm thickness.

Thickness (nm)	55	70	145	185
d (nm)	66	80	116	135
$\rho_0(1.5\text{ K})$ ($\mu\Omega\text{ cm}$)	0.63	0.26	0.23	0.16
$\rho_0(T_{\text{comp}})$ ($\mu\Omega\text{ cm}$)	0.92	0.68	0.58	0.3
$\rho_0(\text{RT})$ ($\mu\Omega\text{ cm}$)	3.83	3.04	3.31	3.04
$\Delta_{tl}(T_{\text{comp}})$	0.94×10^{-3}	0.75×10^{-3}	1.3×10^{-3}	1.4×10^{-3}
$r(T_{\text{comp}})$ ($\Omega\text{ m}^2$)	5.7×10^{-19}	4.1×10^{-19}	8.7×10^{-19}	5.7×10^{-19}

ture because of the large internal fields within ferromagnetic domains even in the absence of externally applied fields. The Lorentz MR is larger for fields (and hence magnetization) transverse to the current, while spin-orbit coupling (AMR) leads to larger in-plane resistivity for magnetization parallel to the current.²¹ More quantitatively, the Lorentz MR is an even function of $B/\rho \sim \omega_c \tau$, the cyclotron frequency times the relaxation time, where B is the internal field in the ferromagnet; $B = 4\pi M + H - H_d$, H the applied field and H_d the demagnetization field. With the film magnetization oriented in plane, the internal field for Co is $4\pi M = 1.8\text{ T}$. To determine the $H=0$ resistivity anisotropy, the MR data above the saturation field are fit to $aB^2 = a(4\pi M + H - H_d)^2$, with fitting parameter a . These fits and their extrapolation to $H=0$ are shown in Fig. 3. In Fig. 3(b) it is seen that the in-plane resistivity anisotropy is nearly zero ($R_{L,0} = R_{T,0}$) at 85 K, which we denote the compensation temperature T_{comp} . At lower temperature $R_{T,0}$ is greater than $R_{L,0}$ [Fig. 3(c)].

At the compensation temperature differences in CPW and CIW resistivities due to in-plane resistivity anisotropy should approach zero, as changing the orientation of the DW's rotates the flux closure caps, yet will produce no change in film resistivity. In Fig. 3(b) a small difference in CPW and CIW resistivities is observed, $\Delta_{tl} = 9 \times 10^{-4}$. Further, while the resistivity anisotropy changes sign and becomes larger in magnitude with decreasing temperature (Fig. 5), Δ_{tl} is always positive. This implies that the difference between CPW and CIW resistivities is not due simply to resistivity anisotropy, which would be proportional to $R_{L,0} - R_{T,0}$. This is illustrated in Fig. 5 in which the difference in in-plane resistivity anisotropy and Δ_{tl} are plotted versus temperature.

The greater CPW resistivity is consistent with a small additional resistivity due to DW scattering, however, there is also other possible physical explanation for this result, which we discuss below. First, to get an idea of the the order of magnitude of any intrinsic DW scattering contribution to the resistivity, we assume that Δ_{tl} at T_{comp} is due to DW scattering. Since walls will be much more effective at increasing resistivity when arranged perpendicular to the current, we further assume DW's have only a small effect on resistivity when parallel to the current.²⁴ The DW interface resistivity is

then given by $r = (d/\delta)\Delta_{tl}\rho_0\delta = \Delta_{tl}\rho_0d$, where d is the domain size, δ is the wall width ($\sim 15\text{ nm}$) and ρ_0 is the film resistivity. Table I summarizes the MR measurements at the compensation temperature and these estimations for different wire thicknesses. For the films studied the average interface resistance is $6 \pm 2 \times 10^{-19}\text{ }\Omega\text{ m}^2$ at T_{comp} and the MR due to the DW material, $\Delta\rho_{\text{wall}}/\rho_0 = (d/\delta)\Delta_{tl}$, is 0.5%. For comparison, these values are approximately a factor of 100 smaller than the Co/Cu interface resistance and MR in GMR multilayers with current perpendicular to the plane of the layers.²⁵

Another mechanism which could produce the observed offset between CPW and CIW resistivities involves the Hall effect.² Both the ordinary Hall effect and anomalous Hall effect in ferromagnetic materials lead to an angle between the current and the electric field in the sample. The ordinary Hall effect in zero applied field, is again associated with the large internal fields within ferromagnetic domains. For the CPW geometry the electric field will be normal to the DW's, except in a very narrow region near the sample boundaries (within about a domain width, 100 nm). For this reason there will be a deflection of the current in the sample. As the Hall angle changes sign in alternating magnetization domains, the current will zigzag through the sample. Berger found that this mechanism would lead to $R_{\text{CPW}} - R_{\text{CIW}} \approx (\omega_c \tau)^2$.² Interestingly, at 85 K for the 55-nm-thick film we estimate this to be 4×10^{-4} , about half the observed difference.

In summary, the large negative MR at room temperature for fields applied along the easy axis of hcp Co films with stripe domains is due to the film micromagnetic structure and ferromagnetic resistivity anisotropy. The temperature dependence of the difference between CPW and CIW resistivities shows that the intrinsic effect of DW interface scattering is at most a small effect on the resistivity of such a stripe domain material. The Hall effect may be important to explaining the observed offset between CPW and CIW resistivities.

The authors thank Peter M. Levy for helpful discussions of the work and comments on the manuscript. We thank M. Ofitserov for technical assistance. This research was supported by DARPA-ONR, Grant No. N00014-96-1-1207. Microstructures were prepared at the CNF, Project No. 588-96.

*Author to whom correspondence should be addressed. Electronic address: andy.kent@nyu.edu

¹See G. R. Taylor, A. Isin, and R. V. Coleman, Phys. Rev. **165**, 621 (1968), and references therein.

²L. Berger, J. Appl. Phys. **49**, 2156 (1978).

³M. Viret, D. Vignoles, D. Cole, J. M. D. Coey, W. Allen, D. S. Daniel, and J. F. Gregg, Phys. Rev. B **53**, 8464 (1996).

⁴J. F. Gregg, W. Allen, K. Ounadjeh, M. Viret, M. Hehn, S. M. Thomson, and J. M. D. Coey, Phys. Rev. Lett. **77**, 1580 (1996).

⁵U. Rüdiger, J. Yu, S. Zhang, A. D. Kent, and S. S. P. Parkin,

- Phys. Rev. Lett. **80**, 5639 (1998).
- ⁶K. Mibu, T. Nagahama, T. Ono, and T. Shinjo, Phys. Rev. B **58**, 6442 (1998).
- ⁷D. Ravelosona, A. Cebollada, F. Briones, C. Diaz-Paniagua, M. A. Hidalgo, and F. Batallan, Phys. Rev. B **59**, 4322 (1999).
- ⁸K. Hong and N. Giordano, Phys. Rev. B **51**, 9855 (1995).
- ⁹Y. Otani, K. Fukamichi, O. Kitakami, Y. Shimada, B. Pannetier, J.-P. Nozieres, T. Matsuda, and A. Tonomura, in *Magnetic Ultrathin Films, Multilayers and Surfaces-1997*, edited by J. Tobin, D. Chambliss, D. Kubinski, K. Barmak, R. Dederichs, W. de Jonge, T. Katayama, and A. Schul, MRS Symposia Proceedings No. 475 (Materials Research Society, Pittsburgh, 1997).
- ¹⁰G. Tatara and H. Fukuyama, Phys. Rev. Lett. **78**, 3773 (1997).
- ¹¹Y. Lyanda-Geller, I. L. Aleiner, and P. M. Goldbart, Phys. Rev. Lett. **81**, 3215 (1997).
- ¹²P. M. Levy and S. Zhang, Phys. Rev. Lett. **79**, 5110 (1997).
- ¹³M. Hehn, S. Padovani, K. Ounadjela, and J. P. Bucher, Phys. Rev. B **54**, 3428 (1996).
- ¹⁴C. Kooy and U. Enz, Philips Res. Rep. **15**, 7 (1960).
- ¹⁵L. D. Landau and E. Lifshitz, Phys. Z. Sowjetunion **8**, 153 (1935).
- ¹⁶C. Kittel, Phys. Rev. **70**, 965 (1946).
- ¹⁷See, for example, A. Hubert and R. Schaefer, *Magnetic Domains* (Springer, New York 1998).
- ¹⁸U. Ebels, P. E. Wigen, and K. Ounadjela, Europhys. Lett. **46**, 94 (1999).
- ¹⁹M. Scheinfein and J. L. Blue, J. Appl. Phys. **69**, 7740 (1991).
- ²⁰A. Aharoni, *Introduction to the Theory of Ferromagnetism* (Clarendon Press, Oxford, 1996).
- ²¹R. McGuire and R. I. Potter, IEEE Trans. Magn. **MAG-11**, 1018 (1975).
- ²²See, e.g., I. A. Campbell and A. Fert, in *Ferromagnetic Materials*, edited by E. P. Wohlfarth (North-Holland, Amsterdam, 1982), Vol. 3.
- ²³At room temperature we estimate the electron mean free path to be 30 nm.
- ²⁴For example, in the model of Ref. 12, a ratio of CPW to CIW MR due to DW scattering is 7 (see their Eq. 21), for a spin asymmetry appropriate for Co (Ref. 25) $\rho_0^\uparrow/\rho_0^\downarrow=3$.
- ²⁵M. A. M. Gijs and G. E. W. Bauer, Adv. Phys. **46**, 285 (1997).